6-3-2011

Denoising medical imagery using a novel framework

Samuel Peter Kozaitis

Jeetkumar M. Mehta

S. Ponkia

Denoising medical imagery using a novel framework

S. P. Kozaitis, J. M. Mehta and S. Ponkia
Department of Electrical and Computer Engineering
150 W. University Blvd.
Florida Institute of Technology
Melbourne, FL 32901

ABSTRACT

We proposed a novel framework that allows a method optimized for white noise to be used for denoising CT imagery. We considered low-dose x-ray CT imagery where lowering the dose of x-rays results in an increase in quantum noise. We first denoised an image independently several times using different parameters. Then, we selected pixels from those denoised images to form a final composite image. We produced results using block-matching denoising, but in principle other methods could work within this framework, as well. The proposed method was able to better reproduce regions of low-contrast than the conventional BM3D approach.

Keywords: block-matching, clustering, computed tomography, denoising, low-dose, non-Gaussian noise

1 INTRODUCTION

Medical imagery may be corrupted by a variety of different types of noise. In MRI imagery, raw data is complex-valued and corrupted with zero-mean noise with equal variance that ultimately results in a Rican distribution.[1] When the mean of the noise increases, the Rician distribution approaches a Gaussian distribution, and when the mean decreases it eventually approaches a Rayleigh distribution. In calibrated, log-transformed projection data of low-dose CT measurements, the noise was found to be Gaussian but with a nonlinear relationship between the mean and variance that varied with the detector bin.[2] Although x-ray energy-converted counts follow a compound Poisson distribution, it is usually modeled as a simple Poisson distribution where the expectation of the variance is equal to the mean and the variance varies linearly with intensity.[3] Because of the widely different noise properties, a unified denoising approach that would work for different types of noise distributions would be particularly useful.

There have been several attempts to remove noise from medical imagery with some success. For example, a wavelet domain method was proposed for noise filtering of medical images which is applicable to various and unknown types of image noise.[4] The method works by first detecting wavelet coefficients that represent features of interest. This is done in order to empirically estimate the conditional *pdf*s of the coefficients given the useful features and background noise. However, the assumptions involved are not always valid. In another approach, a partial differential equation (PDE) method based on pixel similarity has been applied to MRI images.[5] Based on a pixel's consistency with its neighbors, it is assigned a probability and eventually combined into a PDE as an adjusting factor. Also, additive and multiplicative noise can be reduced by solving the Sylvester–Lyapunov matrix equation numerically.[6] For multiplicative noise, the equation is solved recursively using a fixed point algorithm.

Some of the best performing approaches are based on exploiting redundancy of an image in the spatial domain. For example, the non-local means (NLM) filter depends on a kernel derived from pixels that are not local to the pixel under study.[7] An optimized version of this filter using a blockwise implementation was developed and used for denoising 3-D MRI images.[8] A maximum likelihood estimation method for the NLM filter that is used for Rician noise reduction in magnitude MRI images was also developed.[9] Another variation of the NLM algorithm called the dynamic nonlocal means was used for denoising contrast-enhanced MRI images.[10]

Independent Component Analyses, Wavelets, Neural Networks, Biosystems, and Nanoengineering IX,
edited by Harold Szu, Liyi Dai, Proc. of SPIE Vol. 8058, 805809 · © 2011 SPIE
CCC code: 0277-786X/11/$18 · doi: 10.1117/12.882896

Although primarily developed for additive noise, similar approaches have yielded impressive results. For example, an approach based on clustering regions with geometric similarity was combined with an approach with kernel regression. In this approach, each patch in an image can be expressed as a linear combination of only a few patches.[11] Probably the most successful denoising method uses a block-matching 3-D (BM3D) approach, which also uses similar nonlocal patches of images. It performs a 3-D transform on groups of patches and denoises the groups individually.[12] This approach has been applied to MRI images where an algorithm is used to optimize a cost function for noise removal.[13]

In this paper, we proposed a framework for denoising medical imagery that enabled a method optimized for white noise to denoise CT imagery. We first denoised an image independently several times using different parameters within a method optimized for white noise. Then, we selected pixels from the denoised images to form a final composite image. This approach is in contrast to several region-based methods that use various basis functions or image patches to describe geometric structures such as edges and textures. Our main contribution is a framework which allows us to perform image denoising for image-dependent noise.

2 NOISE MODEL

An effective way to decrease the x-ray dose to a patient is to decrease the intensity of x-rays in a CT scan. However, decreasing the intensity increases noise. The noise in the x-ray source has been described by a Poisson process.[14] After x-rays have transversed a specimen, detectors record the photon count, calibrate the data, and compute the logarithm to generate sinogram data. The noise has been shown to be close to a Gaussian distribution with a nonlinear mean-variance relationship.[14] Based on experimental data, the mean-variance relation was found to be

$$\sigma_i^2(\mu_i) = f_i e^{(\mu_i / T)_i}, \tag{1}$$

where μ_i is the mean of the noise in the ith bin, and T and f_i are system specific but object independent factors.[15] The difference between empirical and theoretical predictions are the factors T and f_i. The variable T is a scale factor in the data calibration process. The factor f_i is a factor adjustable for each detector bin and is related to x-rays not being uniform across the field-of-view and detectors not responding equally to x-ray photons. From experimental results, Eq. 1 has been shown to be an accurate model for the noise description in CT.[16]

In our experiments, we used data from Ref. 16, where values of f_i were determined for a Siemens SOMATOM Sensation 16 CT scanner for five different tube currents {100mAs, 80mAs, 60mAs, 40mAs, 17mAs}. It was found that the plots of f_i were similar and related by the equation

$$f_{i,mAs} = 1/(a + b\, f_{i,100}), \tag{2}$$

where $f_{i,100}$ was the data at 100 mAs, $f_{i,mAs}$ was the data at other values, and a and b were found to be 0.03445 and 0.00932 respectively. The value of a deviated from zero because of measured noise at low mAs levels. This data allowed us to estimate the noise variance of a sinogram at a range of mAs levels.

3 PARALLEL DENOISING

The BM3D approach was developed for additive white noise and is one of the best performing algorithms to date. Here we briefly describe the approach and show how it can be effectively used for medical imagery. The BM3D approach relies on both local and non-local characteristics of an image by initially grouping similar patches or blocks of an image. First, small image blocks are grouped based on their similarity. The blocks are essentially stacked to form a 3-

D array, and this process is repeated so that every portion of the image has been compared. Then, a 3-D transform is performed on each stack of blocks independently. Since the data is highly correlated in one dimension, the transform of the data is sparse and denoising methods provide an effective way to remove noise. After the data has been denoised in the transform domain, it is reconstructed, and the denoised blocks are returned to their original locations. The most important parameter in the BM3D algorithm is the value of the noise variance because it affects the amount of denoising in the 3-D arrays. Because the approach assumes white noise, a constant value for all arrays is typically used, independent of the data. Unfortunately, such an assumption is not valid for many types of medical images because the noise is typically data dependent.

We denoised an image $f(x,y)$ multiple times independently using the BM3D approach. We used a different value of noise variance each time, resulting in N different denoised images that formed a 3-D data array $g(x,y,n)$, where $n = 1, 2, \ldots N$. We filtered the noisy image N times using

$$\sigma_n^2 = h[n], \tag{3}$$

where $h[n]$ was the relationship between the noise variance and the intensity of the image. At each set of spatial coordinates x and y, a column of values existed, one corresponding to each value of variance used for denoising. Our approach was to select the best value of n for each spatial coordinate. The final composite image was the values of n at each value of x and y. Using this approach allowed adjacent pixels in the composite image to be calculated with different noise statistics needed to preserve edges. It also directly addressed the nonstationary characteristics of the noise.

We kept the size of the image patches used for comparison in the BM3D approach small. With so few samples it was not possible to form an accurate model of the underlying noise distribution in each patch. In other words, several distributions could provide a reasonable fit. Therefore, the small block size made our approach only weakly dependent on the noise characteristics and applicable to a variety of environments. Because the precise noise statistics were not needed, we simply chose the best possible value of n to form the composite image.

4 CLUSTERING

Some of the most successful denoising methods consider geometric similar regions. However, because in medical imagery the noise often depends on the image intensity, we were interested in regions that were similar in terms of image intensity. Therefore, we used pixel values as features for clustering. Noisy pixels are not necessarily the best choice for feature selection due to the uncertainty of their values. However, we only needed to determine which of a small number of values of n to use for each pixel. We used a low-pass filter as a preprocessing step before clustering to limit pixel values. After clustering, the image was divided into regions Q_k that contain similar values without any geometric constraint. The preprocessed image was described as a union of regions by

$$f_p(x,y) = \bigcup_{k=1}^{N} Q_n . \tag{4}$$

In addition, we used the L_2 distance for simplicity, although other distance metrics could have been used.

There are many clustering algorithms available; however, we needed one that segmented an image into a reasonable number of levels relatively quickly. Therefore, we chose the well-known K-means algorithm, which is a method that segments an image into a prefixed number of clusters. When using the L_2 norm, the K-means algorithm minimized the squared distance between each pixel and the center of its class.

We used the histogram of the preprocessed image to determine the values in the final composite image. Because each pixel in $f_p(x,y)$ corresponded to a cluster Q_n, the corresponding value of n was used to select the value from $g(x,y,n)$ for every value of x and y. In this way, a value was determined for each spatial location in the final composite image. A schematic diagram of the approach is shown in Fig. 1.

5 RESULTS

We conducted initial experiments with the common phantom image shown in Fig. 2(a). The same image with simulated noise calculated from Eqs. (1) and (2) with a tube current of 17 mAs is shown in Fig. 2(b). We wanted the BM3D approach to be effective when only considering a single value of the variance. Therefore, we calculated its value from an area that corresponded to a constant region in Fig. 2(a). The resulting image is shown in Fig. 3(a). The results using the proposed method with $N = 5$ is shown in Fig. 3(b). Overall, the result due to the conventional BM3D approach appeared to be smoother. However, the contrast in critical regions of the image was significantly less when compared to the denoising results from using our proposed method.

We zoomed into the center portion of the image denoised with the conventional BM3D approach, and that is shown in Fig. 4(a). We also showed the center portion of the denoised images using our proposed approach for $N = 3$, 5, and 7 in Figs. 4(b), 4(c), and 4(d) respectively. In the regions that are supposed to constant, the conventional BM3D approach generally reproduces those regions more accurately than the proposed method. In the regions where multiple segments of the original image seem to overlap, the contrast in the conventional BM3D result is virtually eliminated. In our proposed approach, these regions are more faithfully reproduced as N increases. In addition, the streaks present in the results from the proposed approach are also reduced.

We used a CT image shown in Fig. 5(a) to help evaluate the results of our approach. A noisy version of the image corresponding to a tube current of 40 mAs is shown in Fig. 5(b). Using the conventional BM3D approach resulted in the image in Fig. 5(c) and using the proposed method with $N = 5$ resulted in the image in Fig. 5(d). Although the image due to the conventional approach looks smoother, many of the details are lost. In this evaluation, the proposed approach yields a more accurate representation of the original image.

6 CONCLUSION

We used a novel framework that allowed a denoising algorithm optimized for white noise to be used for denoising CT imagery. We produced results using a block-matching denoising approach, but in principle other methods could work within this framework as well. The proposed method was able to better reproduce regions of low-contrast than the conventional BM3D approach.

7 REFERENCES

[1] Gudbjartsson, H. and Patz, S., "The Rician distribution of noisy MRI data," Magn. Reson. Med., 34, 910-914 (1994).
[2] Wang, J., Li, R., Li, H. and Liang, Z., "Penalized weighted least-squares approach to sonogram noise reduction and image reconstruction for low-dose x-ray computed tomography", IEEE Trans. on Imag. Proc., 25(10), 1272 – 1283 (2006).
[3] Gravel, P., Beaudoin, G., and DeGuise, J. A., "A method for modeling noise in medical images," IEEE Trans. Med. Imag., 23, 1221-1232 (2004).
[4] Pizurica, A., Philips, W., Lemahieu, I. and Acheroy, M., "A versatile wavelet domain noise filtration technique for medical imaging," IEEE Trans. Med. Imag., 22(30), 323-331 (2001).
[5] Jin, R., Song, E., Zhang, L., Lijuan, Z., Xu, X. and Hung, C-C., "Denoising of brain MRI images using modified PDE model based on pixel similarity," proc. SPIE 6914, paper 6914-28 (2008).

[6] Sanches, J. M., Nascimento, J. C. and Marques, J. S., “Medical image noise reduction using the Sylvestor-Lyapuov equation,” IEEE Trans. Imag. Proc., 17(9), 1522-1539 (2008).
[7] Buades, A., Coll, B. and Morel, J., “A non-local algorithm for image denoising,” IEEE Computer Society Conference on Computer Vision and Pattern Recognition, 2, (2005).
[8] Coupe, P., Yger, P., Prima, S., Hellier, P., Kervrann, S. and Barillot, C., “An optimized blockwise nonlocal means denoising filter for 3-D magnetic resonance images,” IEEE Trans. Med. Imag., 27(4), 425-441 (2008).
[9] He, L. and Greenshields, I. R., “A nonlocal maximum likelihood estimation method for Rician noise reduction in MR images,” IEEE Trans. Med. Imag., 28(2), 165-172 (2009).
[10] Gal, Y., Mehnert, A. J. H., Bradley, A. P., McMahon, K., Kennedy, D. and Crozier, S., “Denoising of dynamic contrast-enhanced MR images using dynamic nonlocal menas,” IEEE Trans. Med. Imag., 29(2), 302-310 (2010).
[11] Chatterjee, P. and Milanfar, P., “Clustering-based denoising with locally learned dictionaries,” IEEE Trans. Image Process., vol. 18(7), 1438–1451 (2009).
[12] Dabov, K. A., Foi, A., Katkovnik, V. and Egiazarian, K.,”Image denoising by sparse 3D transform-domain collaborative filtering,” IEEE Trans. on Imag. Proc., 16(8), 2080-2095 (2007).
[13] Pedada, R., Kugu, E., Li, J., Yue, Z. and Shen, Y.,”Parameter optimization for image denoising based on block matching and 3D collaborative filtering,” Proc. SPIE 7259, paper 7259-25 (2009).
[14] Macovski, A., [Medical Imaging Systems], Prentice Hall, New York (1982).
[15] Li, T., Li, X., Wang, J., Wen, J., Lu, H., Hsieh, J. and Liang, Z., “Nonlinear sinogram smoothing for low-dose x-ray CT,” IEEE Trans. on Nucl. Sci., 51(5), 2505 – 2513 (2004).
[16] Wang, J., Lu, H., Liang, Z., Eremian, D., Zhang, G., Wang, S., Chen, J. and Manzlone, J. “An experimental study on the noise properties of x-ray CT sonogram data in Radon space,” Phys. Med. Biol. 53, 3327-3341 (2008).

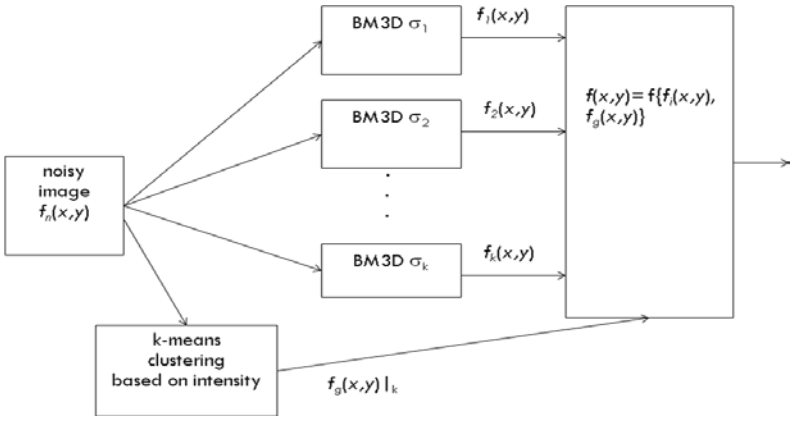

Fig. 1 Block diagram of approach

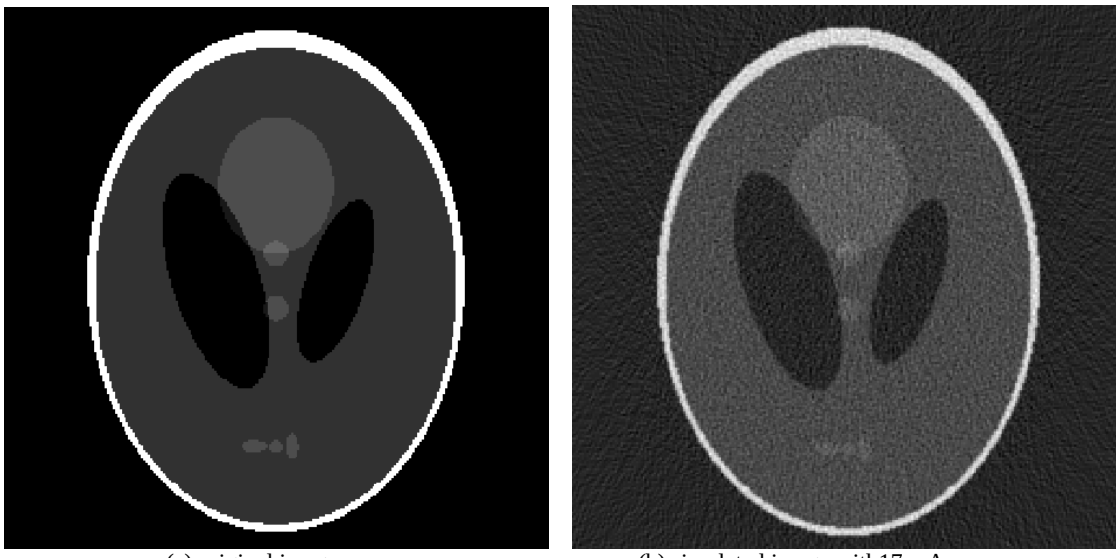

(a) original image (b) simulated image with17 mAs

Fig. 2 Phantom image used in experiments.

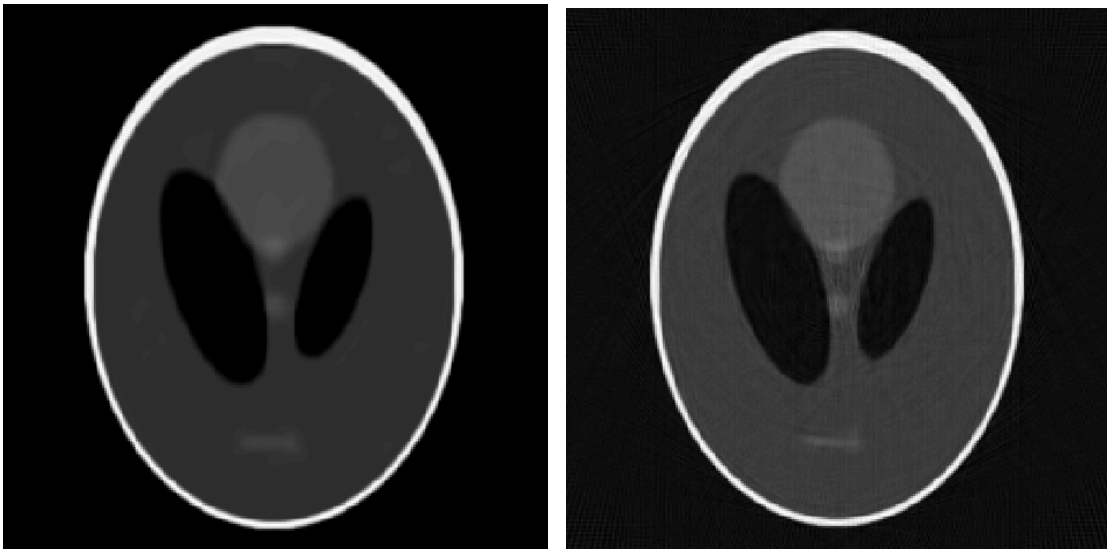

(a) Conventional BM3D algorithm (b) proposed method using $N = 5$

Fig. 3 Denoised phantom image simulated with a tube current of 17 mAs.

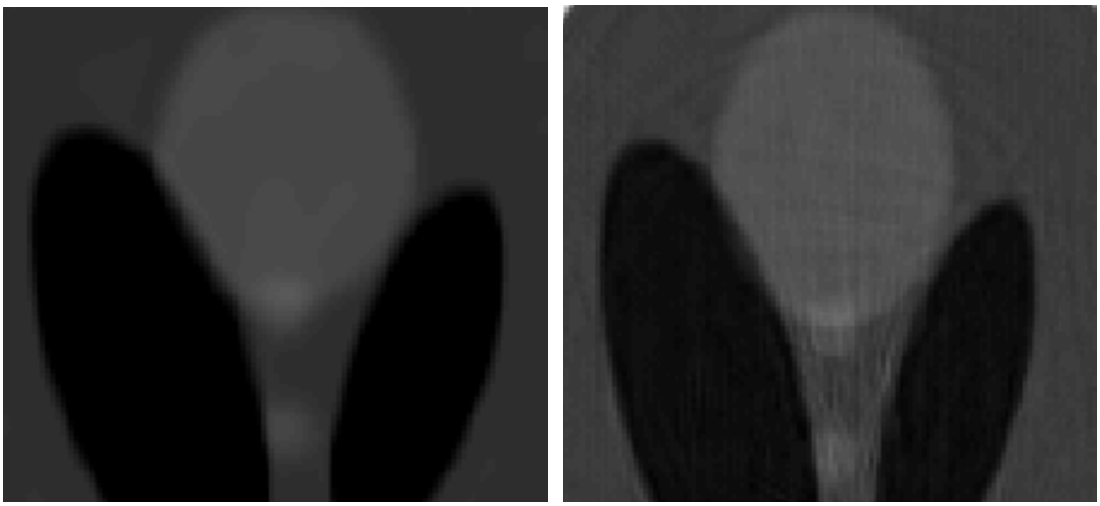

(a) Conventional BM3D approach (b) proposed method using $N = 3$

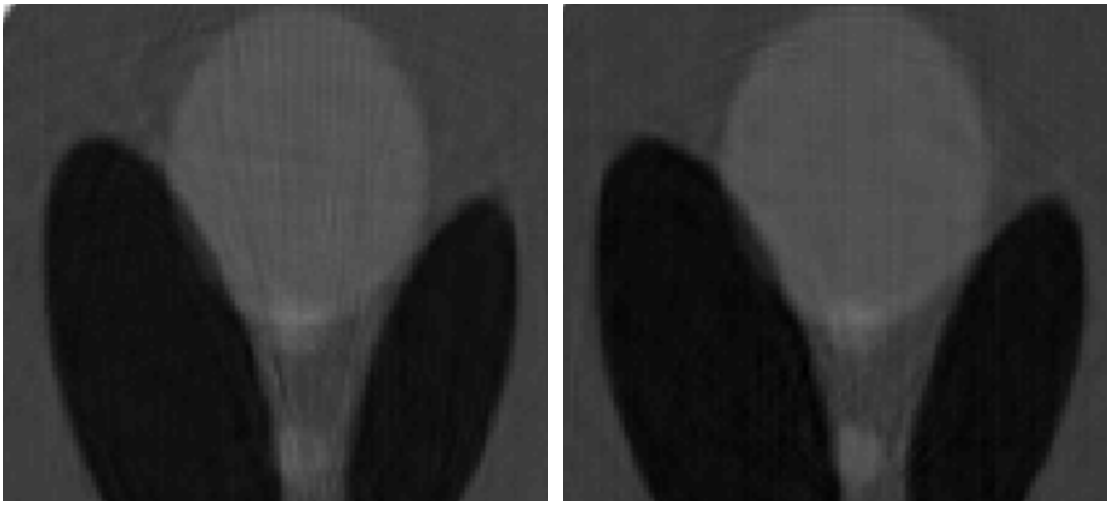

(c) proposed method using $N = 5$ (d) proposed method using $N = 7$

Fig. 4 Center portion of denoised phantom image simulated with a tube current of 17 mAs.

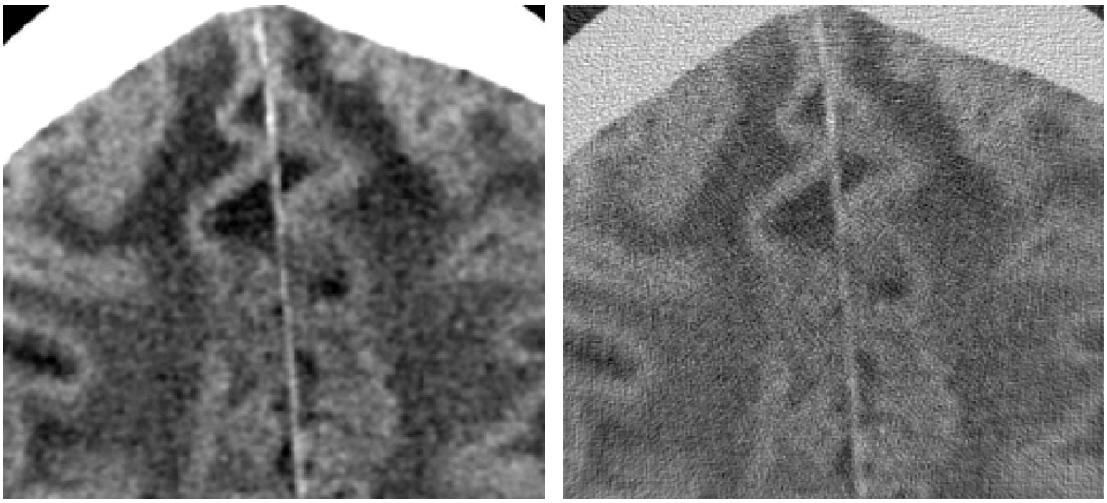

(a) original image

(b) simulated image with 40 mAs

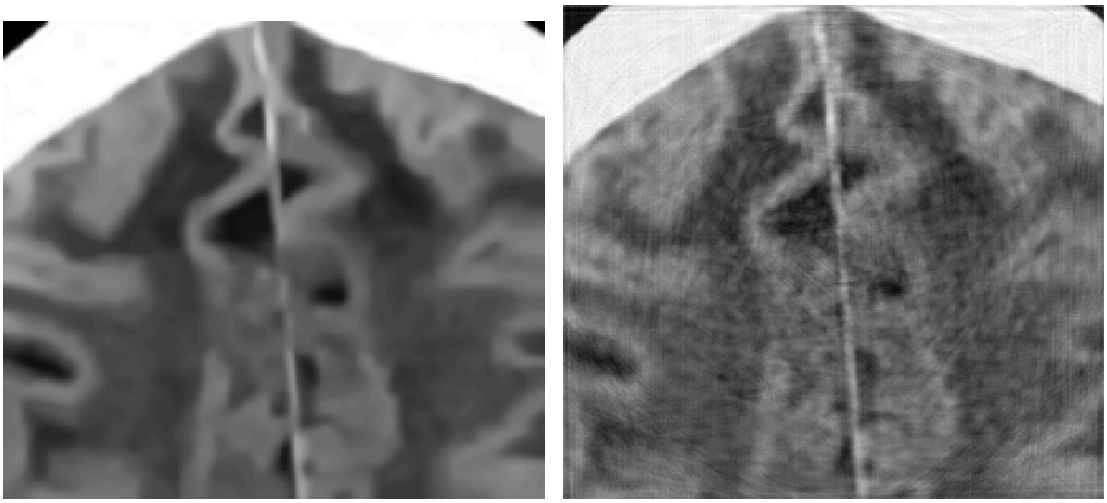

(c) conventional BM3D algorithm

(d) proposed method using $N = 5$

Fig. 5 Denoised CT image simulated with a tube current of 40 mAs.